JOURNAL OF CATALYSIS 85, 63–77 (1984)

The Stoichiometries of H_2 and CO Adsorptions on Cobalt: Effects of Support and Preparation

ROBERT C. REUEL AND CALVIN H. BARTHOLOMEW

BYU Catalysis Laboratory, Department of Chemical Engineering, Brigham Young University, Provo, Utah 84602

Received February 7, 1983; revised July 19, 1983

Catalysts composed of unsupported cobalt and cobalt supported on silica, alumina, titania, magnesia, and carbon were prepared by thermal decomposition, impregnation, precipitation, and evaporative deposition. These catalysts were characterized by high temperature (323–423 K) hydrogen adsorption and conventional 298 K adsorptions of hydrogen and carbon monoxide. Total surface areas of unsupported cobalt catalysts were measured by BET. Metal crystallite sizes were determined independently from XRD, TEM, and hydrogen adsorption. Extents of reduction were measured by O_2 titration at 673 K. Hydrogen adsorption on cobalt is activated and reversible; extents of activation and reversibility vary with support, metal loading, and preparation. The hydrogen adsorption stoichiometry is 1.0 hydrogen atom per surface cobalt atom, if total adsorption at the temperature of maximum uptake is considered. The adsorption of CO is nonactivated and reversible; the stoichiometry for irreversible adsorption varies from 0.4 to 2.3 molecules of CO per surface cobalt atom, depending upon support, metal loading, and preparation. Cobalt dispersion and extent of reduction also vary greatly with support, metal loading, and method of preparation. Cobalt/carbon catalysts prepared by evaporative deposition have unusually high dispersions relative to other cobalt catalysts. Hydrogen adsorption is recommended as the most convenient, reliable technique for measurement of cobalt crystallite size in Co/Al_2O_3, Co/SiO_2, and Co/C catalysts.

INTRODUCTION

Cobalt catalysts find widespread industrial application in hydrogenation and hydrotreating processes. They are also promising candidates for production of fuels and chemicals via Fischer–Tropsch synthesis. Despite their widespread use, there is unfortunately little consensus or basic understanding regarding the measurement of cobalt surface areas or active site densities.

In reviewing the pre-1975 literature dealing with measurements of metal surface areas, Farrauto (*1*) observed that cobalt surface areas had been measured with CO, H_2, and O_2 adsorbates under a variety of conditions using flow and static techniques. He concluded that on the basis of limited previous work and the lack of comparisons with other physicochemical techniques there was no basis for recommending any one technique as being universally acceptable. Unfortunately, there have been no definitive studies of CO or H_2 adsorption on cobalt reported since 1975 which remedy this lack of information. In other words, the adsorption stoichiometries of H_2 and CO on cobalt have not heretofore been determined.

Most of the previous investigations of H_2 and CO adsorptions on cobalt (*1*) involved catalysts which were not well-characterized; for example, extents of reduction to the metallic state and particle-size distributions were usually not measured. Effects of support, metal loading, and preparation were not considered. Yet it is known from recent investigations (*2–5*) that support effects, metal loading, and preparation can greatly influence the stoichiometries of H_2 and CO adsorptions on supported Group VIII metals such as Pt and Ni. In the course

0021-9517/84 $3.00

of this present study, we learned that support, metal loading, dispersion, and preparation influence the stoichiometries of H_2 and CO adsorptions on cobalt. In addition, most of the previous investigators of H_2 adsorption on cobalt did not consider its strongly activated (*6, 7*) and somewhat reversible nature, and thus chose conditions which resulted in less than monolayer coverage.

Thus, the objective of the present investigation was to measure the adsorption stoichiometries of H_2 and CO on well-characterized, supported cobalt catalysts to determine effects of support, preparation, and loading. It was hoped too that this information would provide the basis for development of standard techniques for measuring cobalt surface area. To avoid the complication of activated H_2 adsorption, conditions were carefully chosen for the H_2 adsorption measurements which resulted in saturation coverages on cobalt. Measurements were also made of reversible and irreversible H_2 adsorption uptakes.

EXPERIMENTAL

Catalyst Preparation

The catalysts in this study were prepared by one of three methods: (i) impregnation with an aqueous solution of cobalt nitrate (*5*), (ii) pH-controlled precipitation (*5, 8*), and (iii) evaporative deposition (*9*). The following supports were used: silica (Cab-O-Sil Grade M-5 from Cabot Corp.), alumina (Dispal-M Sample #8032H from Conoco), titania (Oxide P25 from Degussa Inc.), magnesia (Mg-700 from Dart Catalyst Division), carbon (Type UU nut-based, activated carbon from Barnebey and Cheney), and a high purity graphitic carbon (graphitized Spheron from Cabot Corp. which was activated by heating several hours in air at 873 K until 50% of its original weight was lost). An unsupported cobalt was prepared by thermal decomposition of cobalt nitrate at 473 K. Impregnated catalysts of 3 and 10% metal loadings (1, 3, 10, and 15% in the case of Co/Al_2O_3) were prepared for the investigation of metal loading effects. Precipitated 3 wt% Co/SiO_2, Co/Al_2O_3, and Co/TiO_2 were prepared for the investigation of preparation effects. Evaporative deposition was used for preparation of carbon-supported cobalt catalysts, since this technique was previously shown to result in well-dispersed Pt/carbon catalysts (*9*). Our modification of this technique involved vacuum drying of a continuously stirred slurry of the support and a solution of cobalt nitrate dissolved in a 4 to 1 mixture of benzene and ethanol.

Catalyst Reduction

In an earlier study of Ni/Al_2O_3 (*10*), it was shown that carefully controlled decomposition of supported metal nitrates (at low heating rates) in pure H_2 resulted in (i) maximum metal dispersion and (ii) higher reducibility, while preventing exothermic temperature excursions which could sinter the metal crystallites. Based on this previous experience (*10*), the catalysts in this investigation were reduced directly in H_2 at a low heating rate (less than 5 K/min). The heating schedule also included constant temperature pauses of 15–20 min at 373 and 473 K, the temperatures at which water vaporizes and the nitrate decomposes, and with the exception of Co/Al_2O_3 a 16-h hold at 673 K. The reduction of the alumina-supported catalysts included a 20-h hold at 648 K to avoid cobalt aluminate formation (*11–15*). Catalyst samples of 2–3 ml were placed in a flow-through Pyrex cell and reduced in flowing hydrogen (99.99% Whitmore) at a space velocity 2000 h^{-1}. The hydrogen was purified by passing through an Engelhard Deoxo Catalytic purifier followed by a molecular sieve trap at 190 K.

Procedure

Chemisorption measurements. Gas adsorption measurements were performed in a conventional Pyrex glass volumetric adsorption apparatus described in previous studies (*16, 17*). Following reduction, catalyst samples were evacuated at least 30 min to less than 5×10^{-5} Torr and at a tempera-

ture 10–20 K below the reduction temperature. Following evacuation, adsorption isotherms were measured for CO and H_2 at 298 K and for H_2 at the temperature of maximum adsorption (ranging from 298 to 423 K) determined from a companion temperature-programmed desorption study (*7*). Adsorption isotherms were measured by the desorption (decreasing pressure) method after a 45 min equilibration at 300–350 Torr of adsorbate. The total gas uptake was determined by extrapolating the straight-line portion of the adsorption isotherm to zero pressure. Reversible H_2 and CO uptakes were measured following the total uptakes by evacuating to 5×10^{-5} Torr at the adsorption temperature and measuring a second isotherm. The irreversible uptake was determined from the difference between the total gas uptake and reversible uptake. Since irreversible uptakes of H_2 (0–1.0 μmol/g) and CO (0–4.7 μmol/g) on the supports were either negligible or relatively small, no support corrections were made. Extents of reduction were measured by oxygen titration at 673 K according to the method of Bartholomew and Farrauto (*10*), where the reaction of reduced cobalt with oxygen was considered to proceed to Co_3O_4 (*11*). The reproducibility of the adsorption measurements was ±10%.

Calculations of metal dispersion and particle size were carried out in a manner similar to Bartholomew *et al.* (*5, 16, 18*). These calculations were based on the assumption that cobalt metal was present as spherical particles of uniform size, and the assumptions that unreduced cobalt was present in a separate dispersed layer in intimate contact with the support (*11*) and that H_2 uptake on cobalt was activated (i.e., increased with increasing temperature) (*7*). Thus, in calculating metal dispersion (or the fraction of metal atoms exposed), values of H_2 uptake at the temperature of maximum adsorption were used, and metal loadings were multiplied by the fraction of cobalt reduced to the metallic state. Accordingly, percentage dispersion (*%D*) was calculated according to the equation

$$\%D = 1.179X/(Wf) \quad (1)$$

where X = total H_2 uptake in micromoles per gram of catalyst measured at the temperature of maximum adsorption, W = weight percentage of cobalt, and f = fraction of cobalt reduced to the metal determined from O_2 titration. Average crystallite diameters (in nanometers) were calculated from *%D* assuming spherical metal crystallites of uniform diameter d with a site density of 14.6 atoms/nm^2 for supported cobalt crystallites (fcc) (*19–21*) and 11.2 atoms/nm^2 for unsupported cobalt crystallites (hcp) (see Appendix). Thus

$$d = 6.59s/\%D \quad (2)$$

where s = site density in atoms/nm^2 and *%D* = percentage dispersion.

Electron microscopy. Reduced, passivated catalyst samples were crushed to a fine powder, ultrasonicated in n-butanol, and impregnated on fine mesh copper screens coated with holey carbon as outlined by Mustard and Bartholomew (*18*). Transmission electron microscopy (TEM) measurements were made using a Philips EM400HTG electron microscope, with better than 1-nm resolution. The micrograph negatives were photographed at a magnification of 55,000 and enlarged 3 times in printing. The micrographs were then analyzed under a low power microscope with a calibrated eyepiece. Resolution of particles as small as 0.8 nm was possible. For each of the 6 catalysts analyzed by TEM, approximately 1300 crystallites were counted and sized. Surface mean diameters (for comparison with diameters calculated by H_2 adsorption) and volume mean diameters (for comparison with those calculated from X-ray diffraction) were calculated from the crystallite size distribution according to conventional methods (*18, 22, 23*).

X-Ray diffraction line broadening. X-ray powder diffraction (XRD) measurements were performed at the University of Utah using a Philips diffractometer with Cu$K\alpha$ radiation and a graphite monochromator.

Analysis of the line broadening based on the half-maximum breadth of the (111) peak (1/8° 2θ/min scan) according to Klug and Alexander (*24*) and Topsoe (*23*) yielded a volume mean diameter for comparison with TEM results. These calculations included corrections for instrumental broadening, the unresolved $K\alpha_1\alpha_2$ lines, and low-angle reflections.

RESULTS

Typical room temperature hydrogen and carbon monoxide adsorption isotherms are shown in Figs. 1 and 2. Table 1 lists the total and irreversible H_2 uptakes and the irreversible CO uptakes (all measured at room temperature) along with the ratio of the number of CO molecules irreversibly adsorbed per hydrogen atoms irreversibly adsorbed. The room temperature uptakes are average uptakes (up to 5 trials using different samples of the same catalyst) with a precision of better than ±10%.

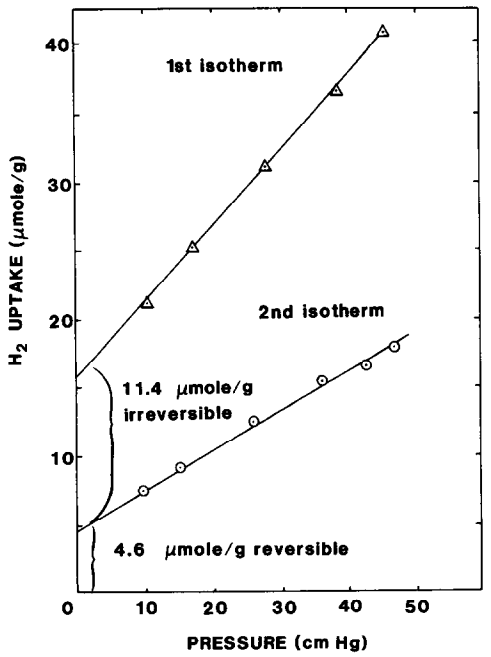

FIG. 1. Reversible and irreversible H_2 adsorption on impregnated 3 wt% Co/SiO_2.

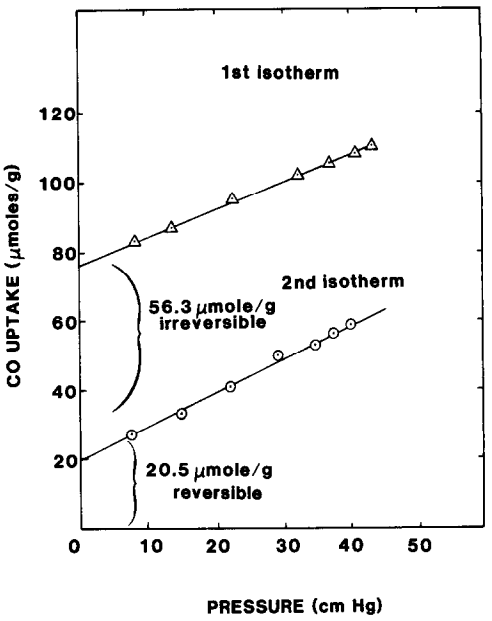

FIG. 2. Reversible and irreversible CO adsorption on impregnated 3 wt% Co/SiO_2.

Total H_2 uptakes on 10 wt% Co/SiO_2 and both types of 10 wt% Co/carbon catalysts are significantly larger (80–121 μmol/g) than the other 10 wt% supported cobalt catalysts (18–24 μmol/g), especially Co/MgO (1.7 μmol/g). Irreversible CO uptakes for the 10 wt% cobalt/carbon catalysts of 199–229 μmol/g are also much larger than those of other catalysts studied.

Three other interesting trends are evident from the room temperature adsorption data: (i) H_2 and CO adsorption uptakes increase with increasing cobalt loading (generally, H_2 uptakes increase approximately linearly with loading in the range of 3–10 wt% cobalt), (ii) the $(CO/H)_{irrev}$ ratio decreases with increasing metal loading, and (iii) catalysts prepared by pH-controlled precipitation have larger $(CO/H)_{irrev}$ ratios than their impregnated counterparts.

It is also evident from these data (Table 1) that the percentage of the H_2 reversibly adsorbed at room temperature on these catalysts is very significant (15–90%). The largest percentages of reversible H_2 adsorption are observed for low loading catalysts

TABLE 1

Uptakes and Stoichiometries for H_2 and CO Chemisorption on Supported and Unsupported Cobalt Catalysts

Catalyst (wt% cobalt)	Total H_2[a] uptake 298 K (μmol/g)	Irreversible[a] H_2 uptake at 298 K (μmol/g)	Irreversible[a] CO uptake at 298 K (μmol/g)	(CO/H)[b] Irrev.	Temperature for maximum H_2 uptake (K)	Total maximum H_2 uptake[c] (μmol/g)	Activation factor A[d]	CO/Co_s[e]
100% Co	22	16	16	0.5	373	22	1.0	0.4
Co/SiO_2								
3	16	11	56	2.5	423	20	1.3	1.3
10	82	70	117	0.8	373	82	1.0	0.7
3[f]	2.1	0.2	5.6	14	398	2.3	1.1	1.2
Co/Al_2O_3								
1	1.5	0.4	2.8	3.5	423	3.2	2.1	0.4
3	3.8	3.0	12	2.0	423	5.6	1.5	1.1
10	24	15	43	1.4	398	29	1.2	0.7
15	37	29	73	1.3	398	37	1.0	1.0
3[f]	6.3	3.6	26	3.6	398	7.8	1.2	1.7
Co/TiO_2								
3	6.1	4.7	11	1.2	348	4.5	1.0	0.9
10	18	14	30	1.1	348	17	1.0	0.8
3[f]	6.4	5.1	21	2.1	413	7.6	1.2	1.4
Co/MgO								
3	0.4	0.2	2.8	7.0	398	0.6	1.5	2.3
10	1.7	0.9	4.0	2.2	398	2.1	1.2	1.0
Co/C (Type UU)								
3[g]	13	5.3	37	3.5	398	18	1.4	1.0
10[g]	121	71	199	1.4	398	143	1.2	0.7
Co/C (Spheron)								
3[g]	17	9.1	43	2.4	398	21	1.2	1.1
10[g]	80	50	229	2.3	398	84	1.0	1.4

[a] Data shown are averages of 2–5 runs for each catalyst; because of negligible support uptake, no correction was made.

[b] Ratio of irreversible uptakes at room temperature.

[c] Data based on one run for each catalyst.

[d] Ratio of maximum H_2 uptake to room temperature H_2 uptake (A = 1.0 is assumed if a ratio is less than 1).

[e] Irreversible CO uptake in molecules per active cobalt metal site, determined from the formula $CO/Co_s = Y/2AX$ where Y = irreversible CO uptake, X = total room temperature H_2 uptake, and A = activation factor.

[f] Controlled-pH precipitation; catalysts not designated were prepared by impregnation.

[g] Evaporative deposition.

(e.g., 1 wt% Co/Al_2O_3) and catalysts prepared by pH-controlled precipitation (e.g., Co/SiO_2). H_2 adsorption is more reversible on Co/Al_2O_3 and Co/carbon than on Co/SiO_2 or Co/TiO_2.

Generally, the adsorption of H_2 above room temperature was greater than that at room temperature due to activated H_2 adsorption (*7*). Table 1 lists room temperature and high temperature hydrogen uptakes and the temperature at which maximum uptake was measured, chosen according to Zowtiak and Bartholomew (*7*). The ratio of maximum to room temperature uptake is defined as the "activation factor" A. Generally, values of A were found to range from 1.0 to 2.1 (see Table 1). In the two cases (3 and 10 wt% Co/TiO_2) where the activation temperature was close to room temperature, the activation factor was assigned the value of 1. Two trends are obvious from the values of A in Table 1: (i) the degree of H_2 activation increases with decreasing cobalt loading (e.g., A = 1.0 for 15 wt% Co/Al_2O_3 and 2.1 for 1 wt% Co/Al_2O_3), and (ii) H_2 adsorption on precipitated catalysts is less activated than on impregnated counterparts. It is also evident from comparison of A values for the 3 wt% cobalt catalysts that H_2 adsorption is more highly activated on Co/Al_2O_3 and Co/MgO than on Co/SiO_2, Co/C, and Co/TiO_2.

The last column in Table 1 lists values of the stoichiometric adsorption ratio for CO on cobalt in molecules of irreversibly adsorbed CO per accessible cobalt surface

atom. The number of accessible surface cobalt atoms was determined from maximum H_2 uptake (i.e., room temperature uptake multiplied by the activation factor), assuming that H_2 adsorption is dissociative and occurs with a stoichiometry of 1 hydrogen atom per surface cobalt atom. The assumption of $H/Co_s = 1$ (Co_s refers to surface cobalt atoms) was verified for unsupported cobalt through comparison of H_2 uptake and BET surface area data (see Table 2 and Appendix) and for supported catalysts through comparison of H_2 adsorption, TEM, and XRD data (as presented below).

Several trends are apparent for the CO/Co_s values in Table 1: (i) they generally decrease with increasing loading, (ii) they are larger for catalysts prepared by controlled-pH precipitation, and (iii) the value of 0.4 for unsupported cobalt is smaller (with one exception) than the values of 0.7–2.3 observed for supported catalysts.

Total H_2 adsorption uptakes, cobalt metal surface areas (calculated from the H_2 uptakes), and BET surface areas of unsupported cobalt catalysts are listed in Table 2. Comparison of metal surface areas determined from H_2 adsorption and BET measurements shows that the stoichiometry of H_2 adsorption on unsupported cobalt metal is 1.0 hydrogen atom adsorbed per available surface cobalt atom.

Representative electron micrographs for cobalt supported on silica, alumina, titania, and carbon (Type UU) are shown in Fig. 3. Histograms of crystallite size distribution determined from the micrographs are presented in Fig. 4. It was necessary to measure metal particles at the fringe of a catalyst sample where the support was thin and translucent. Generally, the cobalt crystallites appeared as dark specks on the large particles of support (see Fig. 3). Cobalt crystallites on titania, however, were diffi-

TABLE 2

H_2 Adsorption Uptakes, BET Surface Areas, and H/Co_s Ratios for Unsupported Cobalt

Catalyst/ pretreatment	H_2 Uptake[a] (μmol/g)	Cobalt surface area[b] (m^2/g)	BET surface area[c] (m^2/g)	H/Co_s[d]
A[e]/Reduced and evacuated 673 K	97.9	10.54	9.72	1.08
A[e]/Reduced 723 K; and evacuated 673 K	27.7 ± 0.3[g]	2.98 ± 0.03	3.46 ± 0.11	0.87 ± 0.02
B[f]/Reduced 773 K; evacuated 750 K	7.39	0.61	0.645	0.95
B[f]/Reduced 773 K; rereduced and evacuated 615 K	5.66 ± 0.46[h]	0.61 ± 0.05	0.645 ± 0.013	0.95 ± 0.08
Average				0.96 ± 0.09

[a] Total H_2 uptake at 298 K.

[b] Calculated from inverse site densities of 8.94×10^{-2} and 6.83×10^{-2} nm^2/atom for hcp and fcc cobalt, respectively (see Appendix). All samples reduced or evacuated below 723 K were assumed to be in the hcp form while Sample B reduced at 773 K was assumed to be in the fcc form.

[c] Determined using argon adsorption at 77 K, assuming 0.146 nm^2/atom.

[d] The ratio of hydrogen atoms adsorbed per surface cobalt atom; determined from the ratio of cobalt surface area to BET surface area.

[e] Prepared by precipitation from a cobalt nitrate solution.

[f] Prepared by calcination of cobalt nitrate at 473 K.

[g] Average of 2 runs.

[h] Average of 3 runs.

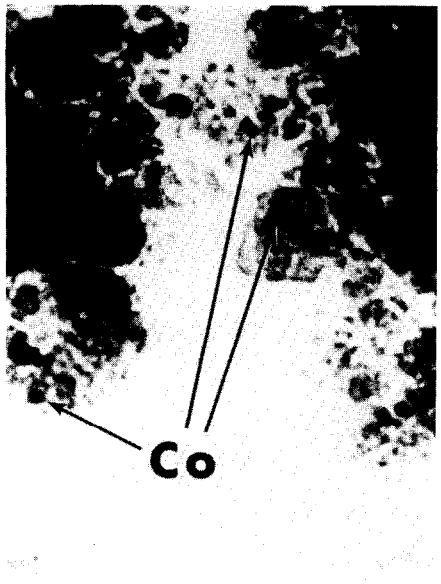

a. 10% Co/SiO_2

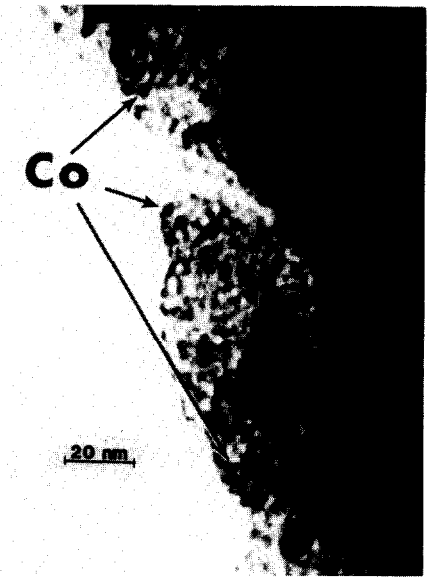

b. 10% Co/C (Type UU)

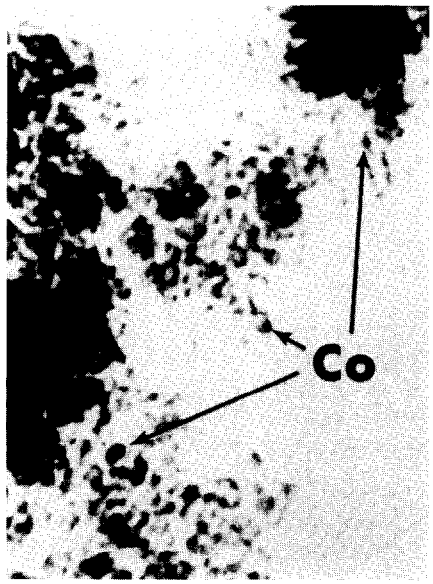

c. 10% Co/Al_2O_3

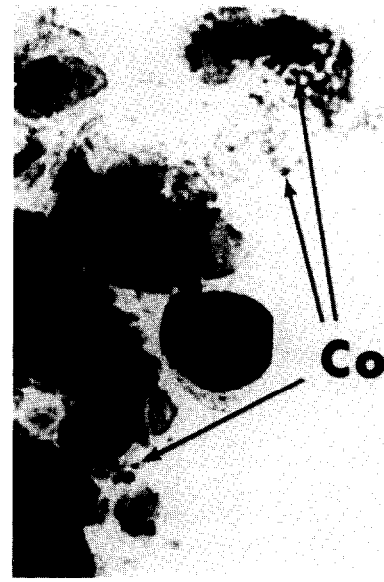

d. 10% Co/TiO_2

FIG. 3. Representative electron micrographs of supported cobalt catalysts.

cult to analyze due to dark spots caused by the overlapping of flat titania plates. Nevertheless, these spots had sharply defined edges and could be distinguished from the somewhat irregular edges of cobalt crystallites. In all of the samples studied, cobalt crystallites appeared to be dense, equiaxed particles. There was no evidence of raft-like structures in Co/TiO_2 as observed previously in Ni/TiO_2 (*18*).

The histograms in Fig. 4 reveal two interesting trends: (i) broader crystallite size dis-

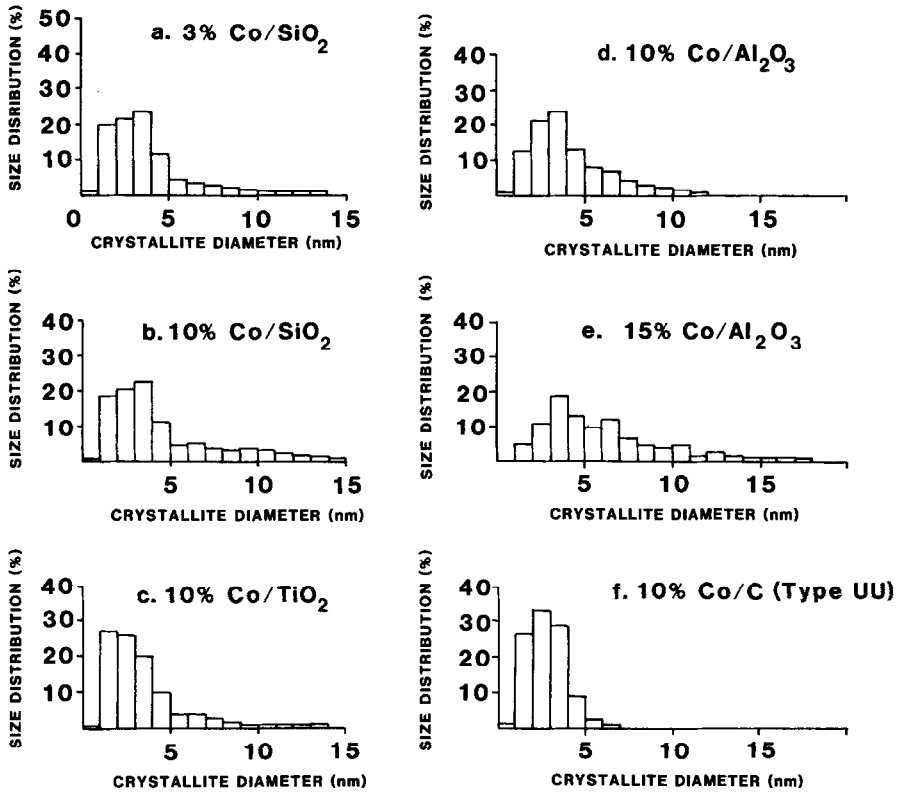

FIG. 4. Histograms of crystallite size distribution for selected supported cobalt catalysts.

tributions occur in catalysts of higher cobalt loading and (ii) significantly smaller crystallites having narrower size distributions are observed for the Co/C catalysts prepared by evaporative deposition.

Table 3 lists values of percentage reduction as determined from O_2 titrations, values of percentage dispersion, and crystallite diameter as calculated from total, maximum H_2 uptakes using Eqs. (1) and (2). From TEM crystallite size distributions, surface mean (d_s) and volume mean (d_v) crystallite diameters were calculated for 3 and 10 wt% Co/SiO_2, 10 and 15 wt% Co/Al_2O_3, 10 wt% Co/TiO_2, and 10 wt% Co/C (Type UU). Mean crystallite diameters are compared in Table 3 with crystallite diameters from H_2 adsorption and XRD. Very good to excellent agreement is evident between values of d_s obtained by H_2 adsorption and TEM for 3 and 10 wt% Co/SiO_2, 3 and 10 wt% Co/Al_2O_3, and 10 wt% Co/C catalysts. Values of d_v from TEM and XRD are in good agreement for samples of 10 wt% Co/SiO_2 and 10 wt% Co/TiO_2. The value of d_s from TEM was a factor of 2 smaller than that from H_2 adsorption in the case of 10 wt% Co/TiO_2. The values of d_v obtained by XRD for the 10 wt% Co/C catalysts were an order of magnitude greater than those measured by TEM or H_2 adsorption.

Several interesting trends are apparent from the extent of reduction and dispersion data in Table 3: (i) the percentage reduction increases, (ii) the percentage dispersion decreases, and (iii) the crystallite diameter increases, all with increasing cobalt metal loading. The precipitated catalysts are less reduced and more highly dispersed than catalysts of similar cobalt loading prepared by impregnation.

TABLE 3

Extents of Reduction, Dispersions, and Average Crystallite Diameters for Supported and Unsupported Cobalt Catalysts

Catalyst (wt% cobalt)	Percentage reduction[c]	Percentage dispersion[d]	Average crystallite diameter (nm)			
			H_2 Adsorption[c] d_s[e]	TEM d_s[e]	TEM d_v[f]	XRD d_v[f]
100% Co	100	0.26	285			
Co/SiO_2						
3	75	11	8.7	11	15	
10	92	10	9.6	12	16	12
3[a]	4.6	20	4.8			
Co/Al_2O_3						
1	11	34	2.8			
3	22	10	9.4			
10	34	9.9	9.7	11	15	
15	44	6.6	14	14	17	
3[a]	16	19	5.0			
Co/TiO_2						
3	14	17	5.6			
10	47	4.5	21	8.7	11	13
3[a]	12	25	3.8			
Co/MgO						
3	11	2.1	45			
10	13	1.9	51			
Co/C (Type UU)						
3[b]	13	55	1.7			
10[b]	47	36	2.7	3.4	3.8	20
Co/C (Spheron)						
3[b]	9.3	89	1.1			
10[b]	15	66	1.5			54

[a] Controlled-pH precipitation; catalysts not designated were prepared by impregnation.
[b] Evaporative deposition.
[c] Calculated from O_2 titration of reduced sample at 673 K, assuming formation of Co_3O_4 (*11*).
[d] Based on total activated H_2 uptake; calculated from Eq. (1).
[e] Surface mean diameter.
[f] Volume mean diameter.

DISCUSSION

H_2 Adsorption on Cobalt: Effects of Support and Preparation on Stoichiometry, Reversibility, and Degree of Activation

This investigation is the first comprehensive study of H_2 and CO adsorption stoichiometries of cobalt and the effects of metal-support interactions on these stoichiometries. Earlier studies (*25–29*) used H_2 adsorption to determine cobalt surface areas for catalysts based on the assumption of an adsorption stoichiometry of 1 hydrogen atom per cobalt surface atom (H/Co_s = 1). Our study demonstrates that this assumption is valid for unsupported polycrystalline cobalt through comparison of H_2 chemisorption and BET adsorption data and for supported cobalt (Co/Al_2O_3, Co/SiO_2, and Co/C) through comparison of cobalt crystallite diameters calculated from H_2 adsorption, XRD, and TEM.

Although cobalt crystallite diameters determined from hydrogen adsorption were in good agreement with those from TEM for

silica-, alumina-, and carbon-supported cobalt systems (see Table 3), the value of d_s from H_2 adsorption was a factor of 2 larger in the Co/TiO_2 system; suggesting that H_2 adsorption was suppressed (i.e., $H/Co_s < 0.5$). This effect may be due to a strong interaction between cobalt and TiO_2, similar to the strong metal-support interactions (SMSI) reported earlier for Group VIII metals on TiO_2 (*2–5, 18, 30, 31*).

A recent study from this laboratory (*7*) showed that H_2 adsorption on cobalt was strongly activated and that the extent of activation depended upon support and metal loading. The data of this study provide additional evidence that H_2 adsorption is activated. That is, kinetic limitations did not allow the maximum (equilibrium) H_2 uptake to be obtained at room temperature, even after 45 min of static exposure at relatively high H_2 pressure. The degree of this kinetic limitation, i.e., degree of activation, depended upon support, metal loading, and preparation. This effect is particularly important in catalysts of low cobalt loading, low reduction (see Table 1), or catalysts in which strong metal-support interactions greatly influence the kinetics (e.g., Co/ZSM-5 (*7, 32*)). This has important implications for previously reported H_2 uptake data for cobalt catalysts; indeed, reported H_2 uptakes may be low by a factor of 2 or more, and turnover frequencies could be high by factors of 2 or greater. In view of the results of this study, existing techniques for measuring H_2 adsorption on cobalt catalysts must be reevaluated. There are essentially two possibly valid approaches: (i) measurement of total H_2 uptake at the temperature of maximum adsorption or (ii) measurement of total H_2 uptake at 298 K after cooling in H_2 from the reduction temperature as suggested by Amelse *et al.* (*33*).

The data in this study (Table 1) show that H_2 adsorption on cobalt is highly (i.e., 15–90%) reversible at room temperature and that the degree of reversibility is affected by loading, support, and preparation. This means that flow adsorption techniques, e.g., that proposed by Amelse *et al.* (*33*), (which measure only irreversible H_2 uptake) result in values of cobalt surface area 15–90% lower than if all surface cobalt metal sites were considered. It is, therefore, necessary to perform H_2 adsorptions on cobalt catalysts by static techniques.

CO Adsorption on Cobalt: Effects of Support, Metal Loading, and Preparation on Stoichiometry

Although the adsorption of CO on cobalt has received considerable attention (*28, 29, 34–41*), the effects of support, metal loading, and preparation on adsorption stoichiometry have not heretofore been quantitatively considered in a single comprehensive study.

Unlike hydrogen, carbon monoxide adsorption on cobalt catalysts did not increase at elevated temperatures, i.e., was apparently not activated. Therefore, all CO chemisorption measurements were carried out at room temperature.

The data in this study provide evidence of a wide variation in CO adsorption stoichiometry (i.e., 0.4 to 2.3 molecules of CO per cobalt surface atom) with cobalt dispersion, support, metal loading, and preparation (see Table 1). The low CO/Co_s ratio of 0.4 for the unsupported cobalt suggests that on poorly dispersed, polycrystalline cobalt, CO adsorbs primarily in a bridged form (one CO molecule attached to two cobalt atoms) similar to that of unsupported Ni (*5*). The larger CO/Co_s ratios for cobalt dispersed on carriers (see Table 1) might be due to the adsorption of CO in combinations of different configurations, i.e., bridged, linear (one CO molecule per cobalt surface atom), and subcarbonyl (two or more CO molecules per cobalt atom) forms. Previous infrared (ir) and temperature-programmed desorption (TPD) studies confirm the presence of different adsorbed species or adsorption states, the relative distribution of which varies with support and metal dispersion. Heal *et al.* (*36*) assigned the ir bands for CO adsorbed on Co/SiO_2 below

2000 cm^{-1} to bridged carbonyls and those above 2000 cm^{-1} to linear and subcarbonyls. Ansorge and Förster (*38*) assigned the ir bands for CO on Co/SiO_2 at 1900 and 2050–2100 cm^{-1} to bridged and linear carbonyls, respectively. In TPD studies of CO adsorption on single crystal surfaces (*39*) and on supported cobalt (*40, 41*) two or three kinds of adsorbed species or adsorption states were observed. Thus, the variations in CO adsorption stoichiometry in this study may be explained by variations in the distribution of subcarbonyl, linear, and bridged CO surface species similar to those reported for supported nickel (*5, 42*) and rhodium (*43, 44*).

Although CO does adsorb on Co_3O_4 (*34*), the variations in CO adsorption stoichiometry observed in this study were probably not due to adsorption on the oxide since Co_3O_4 is generally easily reduced to the metal (*45*) and would probably not have been present at the reduced surface in significant quantities. The unreduced cobalt in the supported catalysts was likely in the form of a spinel or tetrahedral cobalt such as observed by Chin *et al.* in Co/Al_2O_3 (*45*). In a previous study (*5*), it was observed that nickel aluminate did not adsorb CO or H_2 in significant quantities.

In a previous study of nickel-support interactions (*4*), it was observed that CO/H adsorption ratios increased with increasing extent of metal-support interaction, increasing dispersion, and decreasing extent of reduction. Similar trends (Tables 1 and 3) are observed for supported cobalt catalysts in this study. The increases in $(CO/H)_{irrev}$ ratio apparently result from a combination of increases in the CO/Co_s adsorption stoichiometry and decreases in the fraction of H_2 which is irreversibly adsorbed, as metal loading decreases. The increase in CO/Co_s might be attributed to either (i) a geometric effect resulting from changes in surface structure with decreasing particle size or (ii) a support effect involving an increasingly more intimate electronic interaction between metal crystallite and support with decreasing metal crystallite size. However, close examination of the data in Tables 1 and 3 provides evidence in favor of the latter interpretation. For example, in both Co/SiO_2 and Co/Al_2O_3 systems, the 3 and 10 wt% catalysts have approximately the same crystallite size (~9 nm); however, the CO/Co_s ratios are significantly higher and the extents of reduction significantly lower for the 3 wt% catalysts. The lower extent of reduction is an indication in both 3 wt% catalysts of a more intimate interaction of cobalt with the support. The higher $(CO/H)_{irrev}$ and CO/Co_s values for the 3 wt% catalysts prepared by precipitation relative to those prepared by impregnation (see Table 1) may also be attributed to metal-support interactions since their percentage reductions are lower (especially in 3 wt% Co/SiO_2). Moreover, the precipitated catalysts generally have narrower crystallite size distributions (*4, 46*) which promote a more intimate contact with the support.

Effects of Support and Preparation on Dispersion and Extent of Reduction of Cobalt

In addition to information regarding adsorption stoichiometries and reversibilities, the H_2 adsorption and O_2 titration data in this study provide new information regarding effects of support and preparation on dispersion and extent of reduction to cobalt metal.

The data in Table 3 show that 3–15 wt% Co/Al_2O_3 and Co/SiO_2 catalysts prepared by impregnation have moderate cobalt metal dispersions in the range of 6–11% in agreement with previous studies (*28, 47, 48*). In addition, the data in Table 3 reveal significant variations of cobalt dispersion with metal loading in the Co/Al_2O_3 system, with preparation in the Co/Al_2O_3 and Co/SiO_2 systems, and with support in the Co/TiO_2, Co/MgO, and Co/C systems for which there are no previously reported data. As expected, the dispersion of Co/Al_2O_3 increases with decreasing metal loading; however, the observed dispersion of

34% for the 1% Co/Al_2O_3 is unusually high, as was the 42% dispersion of 1% Ni/Al_2O_3 in a previous study (*4*).

Supports were found to greatly influence cobalt metal dispersion. Indeed, percentage dispersions ranged from a low of 2% in the Co/MgO system to a high of 86% in the Co/Spheron carbon system. The apparently low dispersion of Co/MgO may be a result of (i) suppression of H_2 adsorption or (ii) formation of a stable $CoMgO_2$ surface spinel (*49*). The unexpectedly high dispersions of 36–86% observed for the Co/C catalysts could be the result of a fortuitous combination of preparation technique and the presence of active sites on the carbon ideal for binding with cobalt nitrate precursors.

With the exception of 3 and 10 wt% Co/SiO_2, the extents of reduction to cobalt metal for the supported catalysts were in the range of 5–47%. These relatively low extents of reduction suggest a strong interaction between cobalt and the oxide or carbon supports. The strong interaction of cobalt with oxide supports to form surface and bulk spinels, which are not easily reduced to the metal, is a well-known phenomenon (*11–15*). The trend of decreasing extent of reduction with decreasing cobalt loading was previously observed in the Co/Al_2O_3 system and explained by the formation of a very stable surface cobalt aluminate spinel (*11*). The relatively low extents of reduction observed for cobalt on carbon may be a result of oxygenated groups on the carbon support (*9*) capable of strongly binding base metals in the oxidized state. The extremely low extents of reduction observed for the Co/Al_2O_3 and Co/SiO_2 catalysts prepared by controlled-pH precipitation are likely a consequence of more uniform and intimate interaction of the cobalt with the support to form surface spinels or silicates.

Determination of Cobalt Crystallite Size

In order to determine the stoichiometry of hydrogen adsorption on cobalt catalysts, it was necessary to use independent techniques (i.e., TEM and XRD) to measure metal crystallite size. Accordingly, the data of this study provide a basis for evaluating the applicability of these common techniques (H_2 adsorption, TEM, and XRD) for determination of cobalt particle size on various supports.

TEM has the distinct advantage of providing the most direct measurement of crystallite size, assuming the crystallites can be distinguished from the support. In the cases of cobalt on silica, alumina, titania, and carbon, metal crystallites of greater than 1 nm were readily distinguishable from the support, and thus the calculated diameters are considered to be an accurate measure of cobalt crystallite size to within ±10–20%. In addition to crystallite diameters, TEM provides crystallite size distributions and morphological characteristics such as shape and texture. The TEM method, however, is very time consuming and tedious in terms of counting and measuring thousands of particles. While the electron microscope is not difficult to use, it is nevertheless an expensive piece of equipment.

H_2 adsorption was the most practical method for measuring supported cobalt particles. Not only was it fast, inexpensive, and convenient, but in most cases its accuracy was comparable with that of TEM. The best correlation was found in the Co/Al_2O_3 system where the diameters determined by both techniques were essentially the same within ±10%. The crystallite diameters determined for the silica and carbon systems were in good agreement (within 10 and 25%). However, the determination of crystallite size from H_2 adsorption was poor (more than 200% high) for the Co/TiO_2 system, apparently because of an SMSI effect which suppressed H_2 adsorption.

The analysis of X-ray diffraction data was simple and rapid, but the results were not as accurate as H_2 adsorption or TEM because of the relatively low signal-to-noise

ratio in the diffraction experiments and because of inherent limitations in the line profile analysis of the data using half-maximum breadth. This apparently led to rather significant errors in the estimates of particle diameters from XRD for the Co/C catalysts. Recent studies (*50, 51*) have demonstrated that slow scan XRD with Fourier analysis can be used with the same accuracy as H_2 adsorption and TEM.

In view of its simplicity and low cost, we recommend H_2 adsorption for the Co/SiO_2, Co/Al_2O_3, and Co/C systems at Co metal loadings above 3 wt% (where H_2 monolayer coverage is clearly obtained). Because less than monolayer coverage of H_2 occurs on Co/TiO_2 we recommend the XRD method for this system. Careful use of these methods should result in crystallite size measurements within 10–30% of the values measured by TEM.

CONCLUSIONS

1. Hydrogen adsorption on cobalt is highly activated, i.e., a greater amount of hydrogen adsorbs with increasing temperature. The degree of activation increases with decreasing metal loading and increasing degree of metal-support interaction; it varies with preparation of the catalyst. Measurement of a complete monolayer requires equilibration in H_2 at an elevated temperature or cooling in H_2 from an elevated temperature.

2. Hydrogen adsorption on cobalt is highly (15–90%) reversible. The degree of reversibility varies with support, metal loading, and preparation. Thus, to measure a complete monolayer, static rather than flow adsorption techniques are required.

3. The adsorption of hydrogen on unsupported and alumina-, silica-, and carbon-supported cobalt occurs with a stoichiometry of 1.0 hydrogen atom per surface cobalt atom, if total adsorption at the temperature of maximum uptake is considered. H_2 adsorption on Co/TiO_2 is apparently less than monolayer, presumably due to strong metal-support interactions.

4. Adsorption of CO on cobalt at 298 K is apparently not activated and less reversible than H_2. The adsorption stoichiometry varies from 0.4 to 2.3 molecules of CO per cobalt surface atom, depending upon support, metal loading, and preparation. This variability in adsorption stoichiometry may be attributed to variations in the relative fractions of bridged, linear, and subcarbonyl species. The bridged species may predominate in poorly dispersed unsupported cobalt, while linear and subcarbonyl species may predominate in well-dispersed supported cobalt catalysts.

5. Cobalt dispersion and extent of reduction to cobalt metal are greatly affected by choice of support, preparation, and metal loading. The extent of reduction is high for Co/SiO_2, moderate for Co/Al_2O_3, Co/TiO_2, and Co/C, and low for Co/MgO. Co/C catalysts prepared by evaporative deposition have unusually high dispersions (36–86%).

6. Of the three methods used to determine cobalt particle size, TEM and H_2 adsorption provided the greatest degree of accuracy for the Co/Al_2O_3, Co/SiO_2, and Co/C systems. Hydrogen adsorption was the most convenient and least expensive technique. TEM and XRD were most reliable in the case of Co/TiO_2.

APPENDIX

Determination of Surface Site Densities for Cobalt Catalysts

Surface site densities are a function of the crystal structure and the distribution of crystallographic planes at the surface (*52*). Generally surface site densities are calculated from an equally weighted average of the planar densities for the lowest index planes, e.g., the (100), (110), and (111) planes for a face centered cubic (fcc) structure (*52*).

In the case of cobalt catalysts, there is a complication, namely the occurrence of two metallurgical phases (*21, 53, 54*), an hexagonal close pack (hcp) structure at temperatures below about 723 K and fcc at

temperatures above about 723 K (*21*). Besides temperature, the cobalt phase transformation depends upon particle size. When the particle size is very small, the stable structure is fcc, even at temperatures below 723 K (*21, 53, 54*). Indeed, previous investigators of supported cobalt (*19, 20*) found X-ray parameters characteristic of fcc. The X-ray patterns for supported cobalt in this study were consistent with this observation.

Accordingly, the surface site density for supported cobalt catalysts was calculated from an equally weighted average of the site densities for the (100), (110), and (111) planes of fcc cobalt. This resulted in a site density of 14.6 atoms/$(nm)^2$ or an inverse site density of 0.0685 nm^2/atom.

In the case of unsupported cobalt catalysts containing significantly larger crystallites, hydrogen uptakes were measured for samples reduced at 615, 723, and 773 K and quenched to room temperature. From the data in Table 2 for Sample B it is apparent that a significantly greater H_2 uptake was obtained after reduction at 773 K compared to reduction at 615 K. This was not a result of a lower extent of reduction to the metal at 615 K since Catalyst B was originally reduced at 773 K. Rather, it was apparently a result of a phase transformation to hcp when this sample was reheated to 615 K. Indeed by assuming an fcc structure for the sample reduced at 773 K and an hcp structure for the same sample rereduced at 615 K we obtained the same value of H/Co_s!

The surface site density of 11.2 atoms/nm^2 for the unsupported catalyst rereduced at 615 K and then quenched was calculated from a weighted average of the site densities for the most dense planes of the hcp structure, namely 2 × (001), 6 × (100), 6 × (110). The weighting was based on the occurrence of these planes in the unit cell in a 2 : 6 : 6 ratio.

ACKNOWLEDGMENTS

The authors gratefully acknowledge financial support from the Department of Energy, Office of Basic Energy Sciences, Division of Chemical Sciences (Contract DE-AC02-81ER10855) and technical assistance by Mr. Bruno Szalkowski, Mr. Kenneth Atwood, Mr. Val Jones, Mr. John Zowtiak, Mr. Travis Bodrero, Dr. Harold Bissell, Dr. Charles Pitt, Dr. William Hess, and Dr. G. Murali Dhar. We are also indebted to Professor Michel Boudart, Stanford University, for sharing with us a sample of the Spheron Carbon.

REFERENCES

1. Farrauto, R. J., *AIChE Symp. Ser.* **70**(143), 9–22 (1975).
2. Tauster, S. J., Fung, S. C., and Garten, R. L., *J. Amer. Chem. Soc.* **100,** 170 (1978).
3. Vannice, M. A., and Garten, R. L., *J. Catal.* **56,** 236 (1979).
4. Bartholomew, C. H., and Pannell, R. B., and Butler, J. L., *J. Catal.* **65,** 335 (1980).
5. Bartholomew, C. H., and Pannell, R. B., *J. Catal.* **65,** 390 (1980).
6. Matsumara, S., Tarama, K., and Kodama, J., *J. Soc. Chem. Ind. (Japan)* **43,** 175 (1940), supplemental binding.
7. Zowtiak, J. M., and Bartholomew, C. H., *J. Catal.* **83,** 107 (1983).
8. Richardson, J. T., and Dubus, R. J., *J. Catal.* **54,** 207 (1978).
9. Bartholomew, C. H., and Boudart, M., *J. Catal.* **25,** 173 (1972).
10. Bartholomew, C. H., and Farrauto, R. J., *J. Catal.* **45,** 41 (1976).
11. Chin, R. L., and Hercules, D. M., *J. Phys. Chem.* **86,** 360 (1982).
12. Greegor, R. B., Lytle, F. W., Chin, R. L., and Hercules, D. M., *J. Phys. Chem.* **85,** 1232 (1981).
13. Kibby, C. L., Pannell, R. B., and Kobylinski, T. P., "Seventh Canadian Symposium on Catalysis, Edmonton, Alberta, Oct. 19–22, 1980," p. 145.
14. Grimblot, J., and Bonnelle, J.-P., *J. Microsc. Spectrosc. Electron.* **1,** 311 (1976).
15. Lo Jacono, M., and Schiavello, M., *Prep. Catal. Proc. Int. Symp.* 473 (1976).
16. Bartholomew, C. H., Final Report to ERDA, FE-1790-9, Sept. 6, 1977.
17. Pannell, R. B., Chung, K. S., and Bartholomew, C. H., *J. Catal.* **46,** 340 (1977).
18. Mustard, D. G., and Bartholomew, C. H., *J. Catal.* **67,** 186 (1981).
19. Hofer, L. J. E., and Peebles, W. C., *J. Amer. Chem. Soc.* **69,** 2497 (1947).
20. Weller, S., Hofer, L. J. E., and Anderson, R. B., *J. Amer. Chem. Soc.* **70,** 799 (1948).
21. Young, R. S., "Cobalt, Its Chemistry, Metallurgy and Uses." Reinhold, New York, 1948.
22. Whyte, T. E., Jr., *Catal. Rev.* **8,** 117 (1973).
23. Topsoe, H., Ph.D. dissertation, Stanford University, November 1972.

24. (*a*) Klug, H. P., and Alexander, L. E., "X-Ray Diffraction Procedures," Chap. 9, pp. 491–538. Wiley, New York, 1954. (*b*) Klug, H. P., and Alexander, L. E., "X-Ray Diffraction Procedures," 2nd ed., Chap. 9, pp. 687–704. Wiley, New York, 1974.
25. Sastri, M. V. C., and Srinivasan, V., *J. Phys. Chem.* **59,** 503 (1955).
26. Sinfelt, J. H., Taylor, W. F., and Yates, D. J. C., *J. Phys. Chem.* **69,** 95 (1965).
27. Yates, D. J. C., Sinfelt, J. H., and Taylor, W. F., *Trans. Faraday Soc.* **61,** 2044 (1965).
28. Vannice, M. A., *J. Catal.* **37,** 669 (1975).
29. Vannice, M. A., *J. Catal.* **50,** 228 (1977).
30. Tauster, S. J., Fung, S. C., Baker, R. T. K., and Horsley, J. A., *Science* **211,** 1121 (1981).
31. Kao, C.-C., Tsai, S.-C., and Chung, Y.-W., *J. Catal.* **73,** 136 (1982).
32. Bartholomew, C. H., Annual Report to DOE, DOE-ET-14809-8, October 5, 1981.
33. Amelse, J. A., Schwartz, L. H., and Butt, J. B., *J. Catal.* **72,** 95 (1981).
34. Pope, D., Walter, P. S., Whalley, L., and Moss, R. L., *J. Catal.* **31,** 335 (1973).
35. Anderson, R. B., Hall, K. W., and Hofer, C., *J. Amer. Chem. Soc.* **70,** 2465 (1948).
36. Heal, M. H., Leisegang, E. C., and Torrington, R. G., *J. Catal.* **51,** 314 (1978).
37. Bridge, M. E., Comrie, C. M., and Lambert, R. M., *J. Catal.* **58,** 28 (1979).
38. Ansorge, J., and Förster, H., *J. Catal.* **68,** 182 (1981).
39. Bridge, M. E., Comrie, C. M., and Lambert, R. M., *Surf. Sci.* **67,** 393 (1977).
40. Cortes, J., and Droguett, S., *J. Catal.* **38,** 477 (1975).
41. Zowtiak, J. M., Weatherbee, G. D., and Bartholomew, C. H., paper in preparation.
42. Rochester, C. H., and Terrell, R. J., *J. Chem. Soc. Faraday 1* **73,** 609 (1977).
43. Yates, D. J. C., Murrell, L. L., and Prestridge, E. B., *J. Catal.* **57,** 41 (1979).
44. Yao, H. C., Japar, S., and Shelef, M., *J. Catal.* **50,** 407 (1977).
45. Chin, R. L., and Hercules, D. M., *J. Catal.* **74,** 121 (1982).
46. Van Dillen, J. A., Geus, J. W., Hermans, L. A. M., and Van Der Meijden, J. "Proceedings, Sixth International Congress on Catalysis," Paper B7, July 1976, London.
47. Bartholomew, C. H., Quarterly Report, DOE-ET-14809-7, (1981).
48. Hossan, M. A., Dalmon, J. A., Renouptez, A. J., and Trambouze, Y., *J. Chim. Phys.-Chim. Biol.* **75,** 231 (1978).
49. Vedrine, J. C., Hollingen, G., and Duc, T. M., *J. Phys. Chem.* **82,** 1515 (1978).
50. Smith, W. L., *J. Appl. Crystallogr.* **5,** 127 (1972).
51. Sashital, S. R., Cohen, J. B., Burwell, R. L., and Butt, J. B., *J. Catal.* **50,** 479 (1977).
52. Anderson, J. R., "Structure of Metalic Catalysts." Academic Press, New York, 1975.
53. Troiano, A. R., and Tokich, J. L., *Trans. Amer. Inst. Miner. Met. Eng.* **175,** 728 (1948).
54. Battelle Memorial Institute, "Cobalt Monograph," Edited by Centre D'Information Du Cobalt, 1960. pp. 75–120.